Intra-Ping Timing Issues in Multistatic Sonar Tracking

Stefano Coraluppi and Doug Grimmett
Anti-Submarine Warfare Department
NATO Undersea Research Centre
Viale S. Bartolomeo 400, 19138 La Spezia, Italy
coraluppi@saclantc.nato.int, grimmett@saclantc.nato.int

Abstract – *In this paper, we examine a retrodiction approach to handle the out-of-sequence measurement (OOSM) problem in active sonar, for both linear and nonlinear representations of target contact information. We find that the retrodiction approach performs well, even with multiple sensors and multi-lag out-of-sequence measurements. In addition, we examine the impact of the use of a ping-time reference for moving-platform sonar operations.*

Keywords: Multi-sensor target tracking, network-centric tracking, active sonar, out-of-sequence measurement (OOSM) problem.

1 Introduction

In active sonar surveillance with a network of sensors, even with perfect network connectivity, the finite speed of travel of sound waves leads to target contacts with out-of-sequence time stamps. This leads to a difficult recursive filtering problem that must be addressed for effective target tracking. A simple approach to address this problem is to approximate the contact time with the ping time at the source, thus removing the need for out-of-sequence processing. A more effective approach is to use a simple retrodiction algorithm as discussed in [1].

In this paper, we examine the retrodiction approach for both linear and nonlinear representations of target contact information. We find that, for geometries of interest, linear (Cartesian) and nonlinear (polar) problem representations lead to similar filtering performance. We find that the retrodiction approach performs well, even with multiple sensors and multi-lag out-of-sequence measurement (OOSM) problems. This allows us to avoid the use of more sophisticated OOSM algorithms that have appeared in the recent literature (see [2-4] and references therein), and to avoid explicitly accounting for the uncertainty in the target measurement time.

2 Problem Formulation

A representative view of a network of deployed active sonar sensors is illustrated in Figure 1. Each sonobuoy contains a GPS sensor, a signal source, and a receiver array of hydrophones. The nominal offsets from the source and the receiver to the GPS sensor are known.

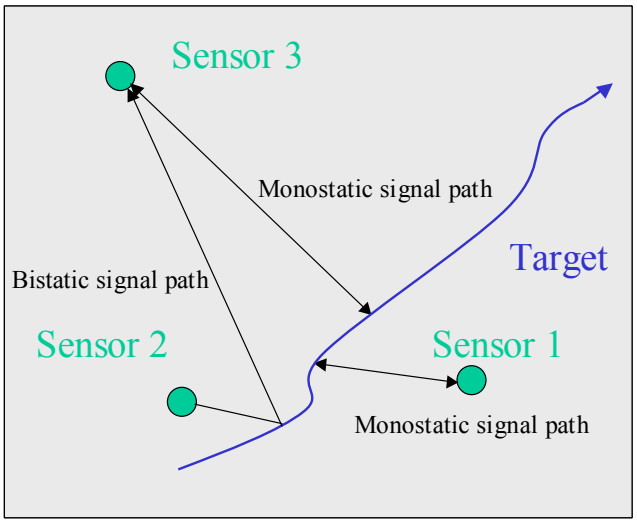

Fig. 1. Network of deployed sonobuoys for active sonar surveillance.

Each sonobuoy has its own ping schedule, with a timing sequence that we denote as $(t_1^n, t_2^n, \ldots)$ for sonobuoy n. In a general multistatic operation, the echoes from each ping are received and processed by each sonobuoy, leading to up to N^2 source-receiver combinations for a field of N sensors. In Figure 1, we have illustrated signal paths for 3 of the 9 possible source-receiver combinations.

After signal processing (filtering, matched filtering, and object formation), the hydrophone data from each (ping, source, receiver) triplet leads to a set of contacts. These contacts include target detections, fixed feature contacts, and false alarms. With communications links among the sonobuoys, all the sets of contacts can be co-located for data fusion and target tracking. The most natural approach is to order the sets of contacts based on the ping times, and to sequentially process these in a multi-sensor tracking algorithm. Active sonar tracking algorithms of varying complexity and performance are described in the literature (see [5-7] and references therein).

Due to the finite speed of sound, the i^{th} ping from the n^{th} sonobuoy, which in our notation occurs at time t_i^n leads to a set of contacts where each has a unique observation time. We denote the observation time for the j^{th} contact as t_{ij}^n. Note that $t_{ij}^n > t_i^n$. This observation time is not

known, though as discussed later we can determine an estimate $\hat{t}_{ij}^{n}$.

Thus, the set of contacts that result from each (ping, source, receiver) triple is such that each contact has a different time stamp. Furthermore, as illustrated in Figure 1, even if multiple sonobuoys ping at the same time, observation times for the same target will different. In particular, source-receiver combinations that include the source that is closest to the target lead to the earlier observation times. Thus, even if contact files are ordered according to ping time for sequential processing in a target tracker, there is a need to address the association and filtering problems for sequences of detections with out-of-sequence measurement sequences

Thus far, to our knowledge, active sonar tracking algorithms have not specifically addressed the OOSM problem, and the observation time for each contact is approximated by the ping time. As we will see, this approximation can lead to a significant increase is track filtering errors for example scenarios of interest, over what is achieved with in-sequence measurement processing.

In Section 3, we describe a number of possible filtering approaches for the active sonar tracking problem. Both Cartesian and polar representations of contact data are considered. With both representations, the contact measurement covariance matrix reflects errors in source location, receiver location, speed of sound, receiver array orientation, contact time, and contact bearing measurements [8]. In addition to in-sequence processing, we consider two OOSM processing approaches. The first is simply to approximate the contact observation time by the ping time, while the second forward-predicts or back-predicts the target state to the time of the current observation to form the filter residual. No process noise is introduced in back-prediction, and the filter remains referenced to the current (most recent) time. As we will see in Section 4, the retrodiction approaches perform almost as well as in-sequence processing.

Our work is described in the context of a field of fixed sonobuoys, though the extension to moving low-frequency active sonar (LFAS) towed arrays is almost immediate. In the latter case, the determination of the estimated observation times $\hat{t}_{ij}^{n}$ must be modified slightly, and care must be taken to use the receiver location at the time of signal reception, rather than at the ping time.

Our retrodiction approach assumes that the estimated observation times $\hat{t}_{ij}^{n}$ are exact. In fact, there are errors in these estimates and these are correlated with the errors in source location, receiver location, speed of sound, receiver array orientation, contact time, and contact bearing measurements. We will neglect the errors in the estimated observation times, as these are small.

In Section 5, we will summarize our work and provide directions for future research.

3 Recursive Filtering

In this section, we first summarize the standard nearly constant velocity target motion model and the Cartesian and polar target measurement models that we use for recursive filtering. We discuss the estimation of target observation times. We provide the equations for the standard linear Kalman filter and nonlinear extended Kalman filters, which are appropriate for in-sequence processing. Finally, we describe the two approaches to OOSM processing that we consider: the first is based on contact observation time approximation, and the second is based on state retrodiction.

3.1 Modeling

The continuous-time 2-dimensional *nearly constant velocity* (NCV) motion model is given by:

$$\dot{X}(t) = F(t)X(t) + w(t), \tag{1}$$

where $X(t) = \begin{bmatrix} x(t) \\ y(t) \\ \dot{x}(t) \\ \dot{y}(t) \end{bmatrix}$, $F(t) = \begin{bmatrix} 0 & 0 & 1 & 0 \\ 0 & 0 & 0 & 1 \\ 0 & 0 & 0 & 0 \\ 0 & 0 & 0 & 0 \end{bmatrix}$, $w(t) = \begin{bmatrix} 0 \\ 0 \\ w_x(t) \\ w_y(t) \end{bmatrix}$,

and $w_x(\cdot)$ and $w_y(\cdot)$ are mutually independent, zero-mean white Gaussian processes with $E\left[w_x^2(t)\right] = q_x\delta(t)$ and $E\left[w_y^2(t)\right] = q_y\delta(t)$.

The initial target state has an unknown target position and a probability distribution for target velocity given by $\left[\dot{x}(0) \quad \dot{y}(0)\right] \sim N(0, \Sigma_0)$.[1] Sensor observations associated with the target are defined at a sequence of non-decreasing times $t_k \in (t_1, t_2, ...)$. It can be shown that discretization of the continuous-time dynamics based on this sequence of times yields the following:

$$X_{k+1} = \Phi_k X_k + w_k, \tag{2}$$

$$X_k = \begin{bmatrix} x_k \\ y_k \\ \dot{x}_k \\ \dot{y}_k \end{bmatrix} = \begin{bmatrix} x(t_k) \\ y(t_k) \\ \dot{x}(t_k) \\ \dot{y}(t_k) \end{bmatrix}, \Phi_k = \begin{bmatrix} 1 & 0 & \Delta t_k & 0 \\ 0 & 1 & 0 & \Delta t_k \\ 0 & 0 & 1 & 0 \\ 0 & 0 & 0 & 1 \end{bmatrix}, \ \Delta t_k = t_{k+1} - t_k, \tag{3}$$

where $\{w_k, k \geq 1\}$ is a zero-mean white Gaussian process, and $w_k \sim N(0, Q_k)$ with

[1] We initialize the filter with uncorrelated speeds in both the *x* and *y* directions and a 1m/s standard deviation in each direction.

$$Q_k = \begin{bmatrix} \frac{1}{3}q_x(\Delta t_k)^3 & 0 & \frac{1}{2}q_x(\Delta t_k)^2 & 0 \\ 0 & \frac{1}{3}q_y(\Delta t_k)^3 & 0 & \frac{1}{2}q_y(\Delta t_k)^2 \\ \frac{1}{2}q_x(\Delta t_k)^2 & 0 & q_x\Delta t_k & 0 \\ 0 & \frac{1}{2}q_y(\Delta t_k)^2 & 0 & q_y\Delta t_k \end{bmatrix}. \quad (4)$$

Our target motion model accounts for maneuvers through the process noise term in (2). The process noise parameters can be increased to model a highly maneuverable target. There is a vast literature on precision modeling of targets that encompasses work on air and ground targets in addition to underwater targets. This work includes multiple-model approaches, higher order models with Gauss-Markov acceleration sequences, the Integrated Ornstein-Uhlenbeck model, and others [9-10]. For targets that are not highly maneuverable and whose motion does depend significantly on the environment, the NCV model is adequate.

The polar representation of sensor measurements available at times $t_k \in (t_1, t_2, ...)$ is given by:[2]

$$Z_k = \begin{bmatrix} r_k \\ \theta_k \end{bmatrix} = h\left(X_k, X_k^R\right) + v_k, \quad (5)$$

$$v_k \sim N(0, R_k), \; R_k = \begin{bmatrix} \sigma_r^2 & \sigma_{r\theta} \\ \sigma_{r\theta} & \sigma_\theta^2 \end{bmatrix}, \quad (6)$$

$$h\left(X_k, X_k^R\right) = \begin{bmatrix} h_1\left(X_k, X_k^R\right) \\ h_2\left(X_k, X_k^R\right) \end{bmatrix} = \begin{bmatrix} \left\| \begin{bmatrix} x_k \\ y_k \end{bmatrix} - \begin{bmatrix} x_k^R \\ y_k^R \end{bmatrix} \right\|_2 \\ \tan^{-1}\left(x_k - x_k^R, y_k - y_k^R\right) \end{bmatrix}, \quad (7)$$

where $X_k^R = \begin{bmatrix} x_k^R \\ y_k^R \end{bmatrix}$ is the measured receiver location at t_k. The determination of the measurement covariance matrix R_k as a function of measurements and measurement error assumptions is discussed in [8]. Note that, for bistatic geometries, this matrix is non-diagonal.

The Cartesian representation of sensor measurements is given by:

$$\begin{bmatrix} \bar{x}_k \\ \bar{y}_k \end{bmatrix} = \begin{bmatrix} x \\ y \end{bmatrix} + v, v \sim N\left(0, \begin{bmatrix} \sigma_x^2 & \sigma_{xy} \\ \sigma_{xy} & \sigma_y^2 \end{bmatrix}\right), \quad (8)$$

where

$$\begin{bmatrix} \bar{x}_k \\ \bar{y}_k \end{bmatrix} = \begin{bmatrix} x_k^R \\ y_k^R \end{bmatrix} + \begin{bmatrix} r_k \cos\theta_k \\ r_k \sin\theta_k \end{bmatrix}. \quad (9)$$

Again, the determination of the measurement covariance matrix as a function of measurement and error assumptions is discussed in [8].

The Cartesian representation of measurement errors introduces a slight localization bias; this bias can be corrected for using the approach discussed in [11]. An extension of this approach to the general bistatic case is discussed in [12].

3.2 Estimation of Observation Times

In the case of successful detection, a ping a time t leads to a target observation at time τ. Given the source location $\begin{bmatrix} x_t^S & y_t^S \end{bmatrix}$, the target location and velocity at time t, and the speed of sound c, the observation time can be determined approximately as follows:

$$c(\tau - t) = \left\| \begin{bmatrix} x_t^S \\ y_t^S \end{bmatrix} - \left(\begin{bmatrix} x_t \\ y_t \end{bmatrix} + (\tau - t) \begin{bmatrix} \dot{x}_t \\ \dot{y}_t \end{bmatrix} \right) \right\|_2, \quad (10)$$

from which we obtain the following:

$$\tau = t + \frac{-b + \left(b^2 - 4ac\right)^{1/2}}{2a}, \quad (11)$$

where $a = \left(c^2 - \left(\dot{x}_t^2 + \dot{y}_t^2\right)\right)$, $b = -2\left(\dot{x}_t\left(x_t - x_t^S\right) + \dot{y}_t\left(y_t - y_t^S\right)\right)$, and $c = -\left(x_t - x_t^S\right)^2 - \left(y_t - y_t^S\right)^2$.

In practice, based on our contact data, we estimate this time difference as follows:

$$\hat{\tau} = t + \xi - \frac{r_k}{\bar{c}}, \quad (12)$$

where ξ is the measured source-to-receiver echo time associated with the sonar contact, $\bar{c}_k$ is the current estimated speed of sound, and $\frac{r_k}{\bar{c}}$ is an estimate of the time from the target observation to signal reception at the receiver. Note that errors in r_k are correlated with errors in ξ and in $\bar{c}_k$, as well as with errors in estimated source and receiver locations, hydrophone array orientation, and the contact bearing measurement [8].

With typical system and measurement errors, we will see in Section 4 that the error between the estimated target observation time $\hat{\tau}$ and the true observation time τ is quite small. Thus, rather than accounting for inaccuracies in the estimated observation time $\hat{\tau}$, we will treat this quantity as exact in our recursive filtering algorithms.

[2] For convenience, in this section we have dropped the superscript and second subscript from the time notation used previously.

This avoids the need for total least squares algorithms to be brought to bear on the problem.

3.3 In-Sequence Processing

We assume that the measurement sequence has been time ordered. That is, the sequence with time stamps $(\hat{\tau}_1, \hat{\tau}_2, ...)$ is re-ordered and results in a sequence with non-decreasing time stamps $(t_1, t_2, ...)$. We denote this as an *in-sequence measurement* (ISM) problem. Optimal MMSE (*minimum mean squared error*) estimates at the measurement times $(t_1, t_2, ...)$ are well-approximated by a maximum likelihood estimate based on the first sensor measurement, followed by recursive filtering computations based on additional measurements using the nonlinear EKF in the case of polar measurements, and the linear KF in the case of Cartesian measurements. The estimate at time t_k is denoted $X(k|k)$ and its covariance is denoted $P(k|k)$.

The maximum likelihood based estimate and covariance are as follows:

$$\begin{bmatrix} x(1|1) \\ y(1|1) \\ 0 \\ 0 \end{bmatrix} = \begin{bmatrix} \bar{x}_1 \\ \bar{y}_1 \\ 0 \\ 0 \end{bmatrix}, \tag{13}$$

$$P(1|1) = \begin{bmatrix} \begin{bmatrix} \sigma_x^2 & \sigma_{xy} \\ \sigma_{xy} & \sigma_y^2 \end{bmatrix} & \begin{bmatrix} 0 & 0 \\ 0 & 0 \end{bmatrix} \\ \begin{bmatrix} 0 & 0 \\ 0 & 0 \end{bmatrix} & \Sigma_0 \end{bmatrix}. \tag{14}$$

Then, for the case of polar measurements, the recursive EKF equations are as follows:

$$X(k+1|k) = \Phi_k X(k|k), \tag{15}$$

$$P(k+1|k) = \Phi_k P(k|k) \Phi_k' + Q_k, \tag{16}$$

$$C(k+1) = \left. \frac{\partial h(X_{k+1}, X_{k+1}^R)}{\partial X_{k+1}} \right|_{X(k+1|k)}$$

$$= \begin{bmatrix} \frac{x(k+1|k) - x_{k+1}^R}{h_1(X(k+1|k), X_{k+1}^R)} & \frac{y(k+1|k) - y_{k+1}^R}{h_1(X(k+1|k), X_{k+1}^R)} & 0 & 0 \\ -\frac{y(k+1|k) - y_{k+1}^R}{h_1^2(X(k+1|k), X_{k+1}^R)} & \frac{x(k+1|k) - x_{k+1}^R}{h_1^2(X(k+1|k), X_{k+1}^R)} & 0 & 0 \end{bmatrix}, \tag{17}$$

$$L(k+1) = P(k+1|k) C'(k+1) \cdot \left(C(k+1) P(k+1|k) C'(k+1) + R_k \right)^{-1}, \tag{18}$$

$$X(k+1|k+1) = X(k+1|k) + L(k+1) \begin{bmatrix} r_{k+1} - h_1(X(k+1|k), X_{k+1}^R) \\ \mathrm{mod}_{2\pi}(\theta_{k+1} - h_2(X(k+1|k), X_{k+1}^R) + \pi) - \pi \end{bmatrix}, \tag{19}$$

$$P(k+1|k+1) = (I - L(k+1) C(k+1)) P(k+1|k). \tag{20}$$

In the case of Cartesian measurements, equations (17, 19) are replaced by the following:

$$C(k+1) = \begin{bmatrix} 1 & 0 & 0 & 0 \\ 0 & 1 & 0 & 0 \end{bmatrix}, \tag{21}$$

$$X(k+1|k+1) = X(k+1|k) + L(k+1) \begin{bmatrix} \bar{x}_{k+1} - x(k+1|k) \\ \bar{y}_{k+1} - y(k+1|k) \end{bmatrix}. \tag{22}$$

3.4 OOSM Processing

The first OOSM approach that we consider consists simply of approximating the time sequence $(\hat{\tau}_1, \hat{\tau}_2, ...)$ with the non-decreasing time sequence $(\tilde{\tau}_1, \tilde{\tau}_2, ...)$, where each contact measurement time is replaced by the corresponding ping time. Then, we proceed as in Section 3.2. We denote this approach as OOSM-1.

The second approach, that we denote as OOSM-2, is a retrodiction approach as discussed in [1], where when faced with an out-of-sequence measurement, the target state is back-predicted to the measurement time, neglecting process noise and with no adjustment to the state covariance matrix. A related approach introduces an adjustment to the state covariance [13]. In both [1] and [13], the linear measurement model is used; here we consider nonlinear (polar) measurements as well.

Consider the measurement time sequence $(\hat{\tau}_1, \hat{\tau}_2, ...)$, and assume that $\hat{\tau}_{k+1} < \hat{\tau}_k$. The state retrodiction equations are given by:

$$X(k+1|k) = \begin{bmatrix} 1 & 0 & \hat{\tau}_{k+1} - \hat{\tau}_k & 0 \\ 0 & 1 & 0 & \hat{\tau}_{k+1} - \hat{\tau}_k \\ 0 & 0 & 1 & 0 \\ 0 & 0 & 0 & 1 \end{bmatrix} X(k|k), \tag{23}$$

$$P(k+1|k) = P(k|k). \tag{24}$$

The state update is given by equations (15-20) is the nonlinear case, and by equations (15-16, 18, 20-22) in the linear case. In both cases, note the filter time remains $\hat{\tau}_k$.

The advantage of both methods OOSM-1 and OOSM-2 is that they do not require data buffering or pre-processing, nor do they require additional filter memory, as in the more involved OOSM approaches [3-4]. In Section 4, we will establish the near-optimality of method OOSM-2 within the context of scenarios of interest for multi-sensor sonar surveillance.

4 Experimental Results

In this section, we first describe the benchmark problem that we will use to evaluate our in-sequence and out-of-sequence recursive filters, with linear and nonlinear measurement sequences. Next, we examine the accuracy of the time stamp estimation approach described in

Section 3. Finally, we provide a quantitative comparison of filter performance.

4.1 Benchmark Problem

The following benchmark example will be used to test the performance of our recursive filters. We have three sensors, each equipped with a source and a receiver that are nominally in the same location. The three sources operate in non-overlapping frequency bands, and each receiver processes only the signal received from its own source. Thus, we have three nearly monostatic source-receiver pairs. The nominal sonobuoy locations in *x*-*y* are (0, 0), (10km, 0), and (20km, 0). The sonobuoys are synchronized, and ping simultaneously with a one-minute ping repetition time.

We assume that measurement errors are zero mean and uncorrelated. Measurement error statistics are as follows:

- Error in measured propagation time τ from source to receiver: $\sigma_\tau = 0.1\text{sec}$;
- Error in measured bearing θ from receiver to target, relative to array heading: $\sigma_\theta = 1\text{deg}$;
- Error in measured receiver orientation ϕ: $\sigma_\phi = 1\text{deg}$;
- Error in measured receiver location $\begin{bmatrix} x^R \\ y^R \end{bmatrix}$:

$$\begin{bmatrix} \sigma^2_{x^R} & \sigma_{x^R y^R} \\ \sigma_{x^R y^R} & \sigma^2_{y^R} \end{bmatrix} = \begin{bmatrix} (10)^2 & 0 \\ 0 & (10)^2 \end{bmatrix} \text{m}^2;$$

- Error in measured source location $\begin{bmatrix} x^S \\ y^S \end{bmatrix}$:

$$\begin{bmatrix} \sigma^2_{x^S} & \sigma_{x^S y^S} \\ \sigma_{x^S y^S} & \sigma^2_{y^S} \end{bmatrix} = \begin{bmatrix} (10)^2 & 0 \\ 0 & (10)^2 \end{bmatrix} \text{m}^2;$$

- Nominal speed of sound c along the sound path: $c = 1500$ m/s; Error in measured speed of sound: $\sigma_c = 15$ m/sec.

Based on measured quantities, we derive the polar and Cartesian measurements and measurement covariance matrices used in equations (5-9). Details are in [8]. Note that each source-receiver pair is not quite monostatic, since measured source and receiver locations are not identical.

For the benchmark problem, we consider a single target traveling through the sensor field. Thus, whether in polar or Cartesian coordinates, we have three target observations per minute. As illustrated in Figure 1, the target starts at (15000km, 40,000km), and moves with velocity (0m/sec, -2.5m/sec) for 10hrs. For OOSM processing, we will arbitrarily process the measurements in a predefined sequence, corresponding to the first, then the second, and then the third sonobuoy. In-sequence processing would require that, depending on the measurements, the second or third sonobuoy contact be processed first, then the other, and finally the first sonobuoy contact. Thus, our OOSM processing will include a fairly complex out-of-sequence ordering.

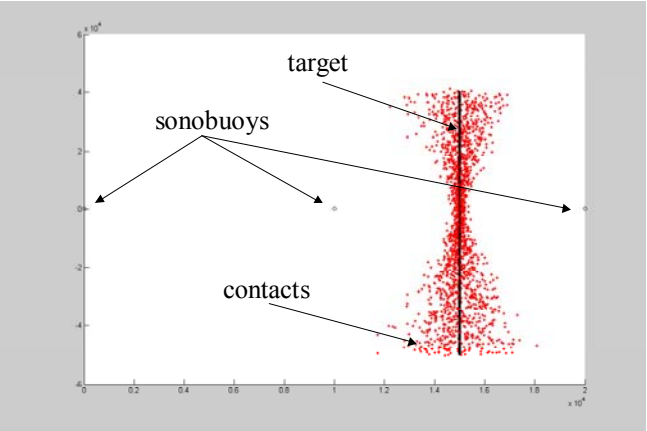

Fig. 2. Visualization of geometry for benchmark problem, with one realization of sonar contacts overlaid. Target motion is in the –*y* direction. The total scale is 20km in the *x*-dimension, and 120km in the *y*-dimension.

The interesting hourglass shape for the distribution of contacts follows from the dependence of the covariance matrix expressions on source-target-receiver geometry [8].

4.2 Accuracy of Observation Time Estimates

Both in-sequence processing and retrodiction-based OOSM processing (OOSM-2) require the determination of the time sequence $(\hat{\tau}_1, \hat{\tau}_2, ...)$, which approximates the *actual* sequence of observation times $(\tau_1, \tau_2, ...)$. For each contact, we use equation (12) to estimate the observation time. The observation time estimation error depends on the measurement errors that we identified previously. For our benchmark problem, given the geometry of the problem and our error statistic assumptions, we find an RMS error of roughly 0.05sec. This is small, and thus we can treat the sequence $(\hat{\tau}_1, \hat{\tau}_2, ...)$ as if it were exact.

A proper accounting for the error in our estimate of observation time would require that, based on equation (12), we derive an expression for the standard deviation of observation time estimation errors. Next, the target state estimation problem would require a total least squares approach. This is particularly complex here, since the estimation error in the observation time is correlated with the error in the polar and Cartesian measurements.

4.3 Filter Comparison

The following list summarizes the recursive filters that we described in Section 3:

- Nonlinear (polar) measurements with in-sequence measurement processing (method NL-ISM, or standard EKF);
- Linear (Cartesian) measurements with in-sequence measurement processing (method L-ISM, or standard KF);
- Nonlinear (polar) measurements with out-of-sequence measurement processing (methods NL-OOSM-1 and NL-OOSM-2);
- Linear (Cartesian) measurements with out-of-sequence measurement processing (methods L-OOSM-1 and L-OOSM-2).

For a single realization of the benchmark problem, in Figures 3-4 we illustrate the sequence of state estimates for the six filters. The actual locations of the sonobuoys and of the target (at the observation times) are in black. The colored lines are the state trajectories.

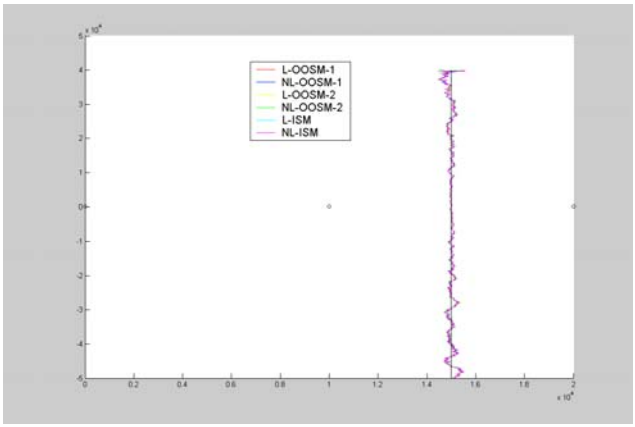

Fig.3. Realization of benchmark problem: state estimate trajectories for the six recursive filtering schemes.

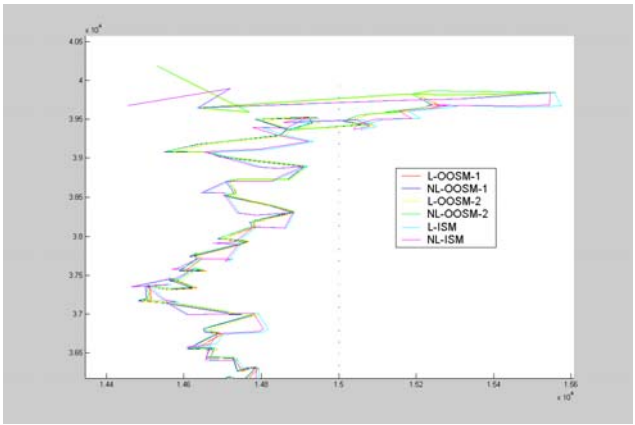

Fig.4. Close-up view of first portion of benchmark problem realization.

The key points to note from Figure 3 are that, from a macroscopic view, all the state trajectories are quite similar, and that estimation errors are larger at the beginning and at the end of the run. The latter point is consistent with the hourglass shape of the distribution of contacts that we noted in Figure 2. In Figure 4, we observe that the in-sequence state trajectories are initialized with a different contact than the OOSM trajectories.

The OOSM trajectories remain quite similar throughout the state sequence realization. Indeed, in order to quantitatively evaluate state estimation accuracy, we consider a Monte Carlo evaluation based on 50 realizations of the contact data. The results are summarized in Table 1 in terms of the RMS error (RMSE) of the state estimates.

Table 1. Monte Carlo based filter comparison.

Filter	RMSE
Input Data	753.50
L-OOSM-1	152.86
NL-OOSM-1	152.71
L-OOSM-2	146.44
NL-OOSM-2	145.26
L-ISM (KF)	145.39
NL-ISM (EKF)	145.22

First, we note that all six filters provide a drastic reduction in localization error as compared with the measured contact data. Next, note that the retrodiction approach (OOSM-2) provides smaller errors that the observation time approximation approach (OOSM-1), and further we find that OOSM-2 performs almost as well as in sequence processing (KF, EKF). Finally, we find that polar representation of contact data leads to slightly lower estimation errors, for all approaches (OOSM-1, OOSM-2, and ISM).

We have repeated the Monte Carlo study for similar benchmark problems, and the numerical performance of the filters supports the same conclusions.

5 Receiver Positioning Errors

At the time of a sonar transmission, the source's position will be known. Between this time and the successive ping transmission, the sonar is waiting for sonar echoes to be received. The ping repetition interval (T_{PRI}) defines how long this time is, and defines the maximum area of search (circular if monostatic, elliptical if bistatic) for the sonar before next-ping interference would be received. During the ping repetition interval, the source, receiver, and target continue to move with some velocity. We wish to quantify how much localization error is introduced by assuming a single time stamp reference for asset positions during the interval. The single time reference can be either relative to the source transmission time, or to the receiver time.

Using only the source transmit time as reference for assets positions, we mis-assume the position of the receiver, as it continues its motion after ping transmission. Therefore the assumed receiver position will have a localization error given by $v_{\mathrm{r}}\tau_{\mathrm{str}}$, where v_{r} is the velocity of

the receiver, and τ_{str} is the intra-ping time delay (after source transmit time) for a sonar echo to arrive at the receiver (sound path of source-target-receiver). We know that depending on the target location the time of echo arrival will vary, and therefore distant targets will allow for more localization in the position of the receiver, than close targets. Of course, higher ship velocities will also increase the localization error. The resulting localization error for this intra-ping timing effect can be studied using the analytic localization expressions with the corresponding values for receiver position error.

Figure 5 shows the localization error image for a bistatic scenario with the following settings: source at (x, y)=(-10, 0) km; receiver at (x, y)=(0, 0) km; surveillance within a 60x60 km box; receiver velocity of 4, 8, 12, and 16 knots.

The results show increasing localization error as the source-target-receiver range increases. The magnitudes of the errors are not very significant compared to typical system localization errors, as long as the receiver speed is small. As the receiver speed increases, the localization error can grow to moderate levels around 200 meters at longer ranges. This result does not take into account other positional, timing, bearing, or speed of sound errors. Note that, unlike the effect of receiver location error analyzed in [8], the increased time mis-alignment with increasing range leads to range-dependent localization errors.

This analysis is based on the localization error analysis discussed in [8]. For each receiver velocity case of interest, we set the receiver measurement covariance in both x and y such that the resulting expected velocity match the assumed velocity. Then, the plots indicate the trace of the measurement covariance matrix at each point in the region, based on receiver positioning errors.

The error for receiver position due to the intra-ping timing effect can be mitigated by mapping each sonar contact with accurate receiver positions that correspond to the arrival times for each echo.

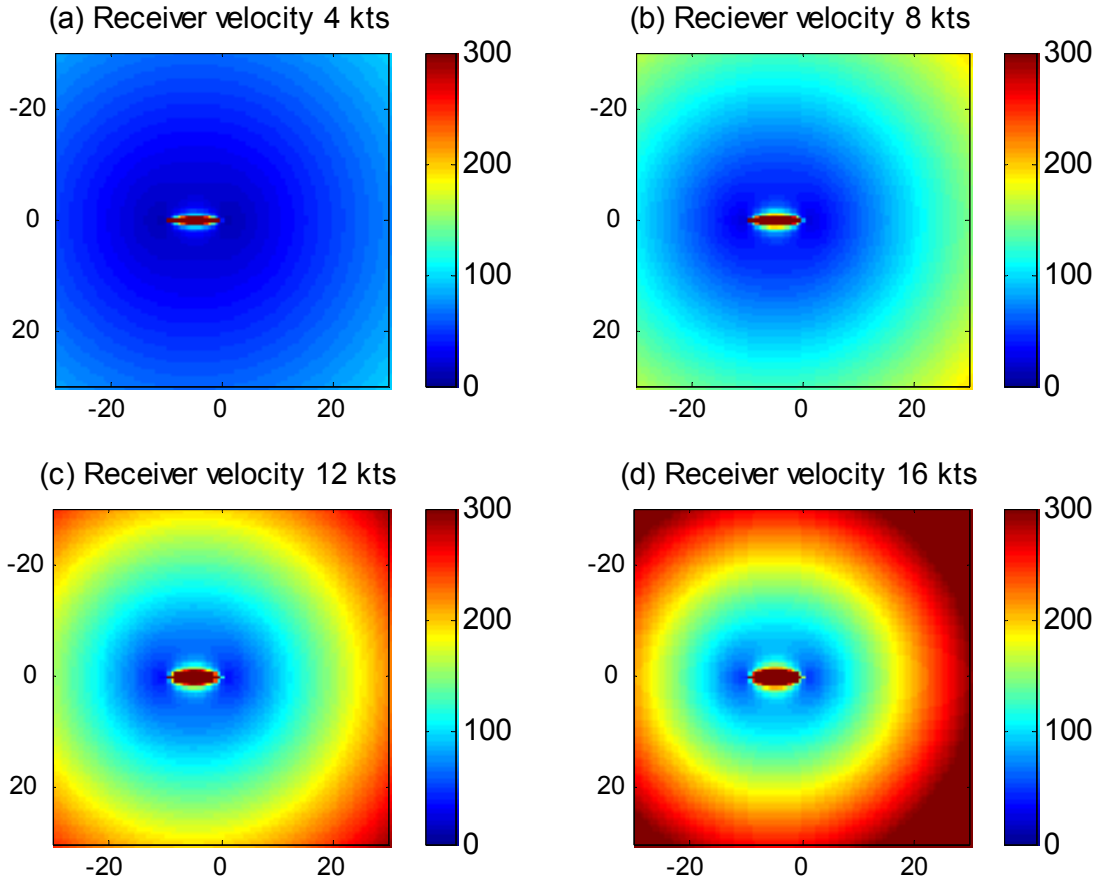

Fig. 5. Target localization error (meters) due to intra-ping receiver motion when using a single time reference (source transmission time) for the entire ping.

In [14], we study the impact of system and measurement errors on the localization of sonar detections, using representative values for system errors as well as representative scenario geometries. In general, the sensitivity analysis shows that for representative low, medium, and high values of the four measurement errors, the bearing error is the dominant effect on localization accuracy, especially at range. The selected values of timing and positional errors did not have as large an effect on localization accuracy. Speed of sound errors can be significant, but they will normally always be dominated by bearing errors. Measurement error values

have been determined which individually yield a mean error (over the whole surveillance area) of 200 meters. Given these results, more localization accuracy is to be gained from improving the bearing measurement error than any other parameter, although this may be the most difficult of the four to improve in practice.

Relative to the impact of system and measurement errors, the localization error due to receiver positioning errors is non-negligible, as it generally produces contact localization errors of a few hundred meters. Thus, it is important to remove these errors with accurate receiver positioning.

6 Conclusions and Future Work

In this paper, we have studied the out-of-sequence measurement problem for active sonar surveillance networks. Due to the finite speed of sound, the ping time does not correspond to the target observation time. Based on the measured contact data, we can estimate the target observation time, as well as develop Cartesian and polar representations of the state measurement equations. We neglect uncertainties in the observation time estimates, as these errors are small.

In addition to a data buffering and in-sequence processing approach, we study two approaches to OOSM recursive filtering. The second of these is a retrodiction approach and it is found to perform almost as well as in-sequence processing, for scenarios and geometries of operational interest. Thus, it appears that the more complex OOSM algorithms that have been developed for radar applications are not required in this context.

The retrodiction-based OOSM filter studied in this paper can be used readily as part of multi-target sonar tracking algorithms. In particular, within a multi-hypothesis tracking framework, we score all track hypotheses based on the filter time, and data association gates are evaluated using predicted or back-predicted state estimates.

Finally, we study the impact of using the source ping time for receiver positioning in moving-platform sonar operations. While the resulting errors are non-negligible, it is straightforward to remove this processing error.

References

[1] S. Blackman and R. Popoli, *Design and Analysis of Modern Tracking Systems*, Artech House, 1999.

[2] R. Hilton, D. Martin, and W. Blair, Tracking with Time-Delayed Data in Multisensor Systems, *NSWCDD/TR-93/351*, Dahlgren, VA, 1993

[3] M. Mallick, S. Coraluppi, and Y. Bar-Shalom, Comparison of Out-of-sequence Measurements Algorithms in Multi-platform Target Tracking, in *Proceedings of the 4th International Conference on Information Fusion*, August 2001, Montreal, Canada.

[4] M. Mallick and A. Marrs, Comparison of the KF and PF Based Out-of-Sequence Measurement Filtering Algorithms, in *Proceedings of the 6th International Conference on Information Fusion*, July 2003, Cairns, Queensland, Australia.

[5] D. Lerro and Y. Bar-Shalom, Interacting Multiple Model Tracking with Target Amplitude Feature, *IEEE Transactions on Aerospace and Electronic Systems*, Vol. 29(2), 1993.

[6] S. Coraluppi and D. Grimmett, Multistatic Sonar Tracking, in *Proceedings of the SPIE Conference on Signal Processing, Sensor Fusion, and Target Recognition XII*, April 2003, Orlando FL, USA.

[7] S. Coraluppi and C. Carthel, Multi-Hypothesis Sonar Tracking, submitted to the *7th International Conference on Information Fusion*, June 2004, Stockholm, Sweden.

[8] S. Coraluppi, Multistatic Sonar Localization Analysis, *NURC Technical Report SR-377*, June 2003.

[9] Y. Bar-Shalom and X. Li, *Multitarget-Multisensor Tracking*, YBS Publishing, 1995.

[10] L. Stone, C. Barlow, and T. Corwin, *Bayesian Multiple Target Tracking*, Artech House, 1999.

[11] D. Lerro and Y. Bar-Shalom, Tracking with Debiased Consistent Converted Measurements versus EKF, *IEEE Transactions on Aerospace and Electronic Systems*, Vol. 29(3), 1993.

[12] S. Coraluppi and C. Carthel, Progress in Multistatic Sonar Localization and Tracking, *NURC Report SR-384*, to appear.

[13] H. Wang, T. Kirubarajan, and Y. Bar-Shalom, Precision Large Scale Air Traffic Surveillance Using IMM/Assignment Estimators, *IEEE Transactions on Aerospace and Electronic Systems*, Vol. 35(1), January 1999.

[14] D. Grimmett and S. Coraluppi, Sensitivity Analysis for Multistatic LFAS Localization Accuracy, *NURC Report SR-386*, to appear.